PROCEEDINGS OF SPIE

SPIEDigitalLibrary.org/conference-proceedings-of-spie

Metastable and scattering states of a diatomic beryllium molecule

Derbov, V., Chuluunbaatar, G., Gusev, A., Chuluunbataar, O., Vinitsky, S., et al.

V. L. Derbov, G. Chuluunbaatar, A. A. Gusev, O. Chuluunbataar, S. I. Vinitsky, A. Góźdź, P. M. Krassovitskiy, I. Filikhin, A. V. Mitin, "Metastable and scattering states of a diatomic beryllium molecule," Proc. SPIE 11846, Saratov Fall Meeting 2020: Laser Physics, Photonic Technologies, and Molecular Modeling, 118460Y (4 May 2021); doi: 10.1117/12.2585634

SPIE.

Event: Saratov Fall Meeting 2020, 2020, Saratov, Russian Federation

Metastable and scattering states of a diatomic beryllium molecule *

V.L. Derbov[a], G. Chuluunbaatar[b,c], A.A. Gusev[b], O. Chuluunbaatar[b,d], S.I. Vinitsky[b,c], A. Góźdź[e], P.M. Krassovitskiy[a,f], I. Filikhin [g], A.V. Mitin[h,i]

[a]N.G. Chernyshevsky Saratov National Research State University, Saratov, Russia
[b] Joint Institute for Nuclear Research, Dubna, Russia
[c] Peoples' Friendship University of Russia (RUDN University), 117198 Moscow, Russia
[d] Institute of Mathematics, National University of Mongolia, Ulaanbaatar, Mongolia
[e] Institute of Physics, University of M. Curie-Skłodowska, Lublin, Poland
[f] Institute of Nuclear Physics, Almaty, Kazakhstan
[g] Department of Mathematics and Physics,North Carolina Central University, Durham, NC 27707, USA
[h] Moscow Institute of Physics and Technology, Dolgoprudny, Moscow Region, Russia
[i] Joint Institute for High Temperatures of RAS, Moscow, Russia

ABSTRACT

The calculations of vibration-rotation bound states and new metastable states of a diatomic beryllium molecule important for laser spectroscopy are presented. The problem is solved using the potential curve and the authors' software package that implements the iteration Newton method and the high-accuracy finite element method. The efficiency of the proposed approach is demonstrated by calculating vibration-rotation bound states and, for the first time, rotation-vibration metastable states with complex- valued energy eigenvalues (with negative imaginary parts of the order of $(10^{-20} \div 6)$ cm^{-1}) in a diatomic beryllium molecule. The existence of these metastable states is confirmed by calculating the corresponding scattering states with real-values resonance energies.

Keywords: laser spectroscopy, eigenvalue problem, bound and metastable states, finite element method, diatomic beryllium molecule, vibration-rotation bound states, rotation-vibration metastable and resonance scattering states

1. INTRODUCTION

During the last decade, theoretical studies[1–5] have shown 12 vibrational bound states in a diatomic beryllium molecule, whereas 11 states were extracted from the experimental data of laser pump-probe spectroscopy (see Fig. 1 in Ref. 6). Earlier[7] we started to study the vibration-rotation spectrum of diatomic beryllium molecule. We solved the boundary value problem (BVP) for the second-order ordinary differential equation (SOODE) with potential function numerically tabulated on a non-uniform grid in a finite interval of the independent variable values.[3] To formulate the BVP on a semiaxis, the potential function should be continued beyond the finite interval using the additional information about the interaction of atoms comprising the diatomic molecule at large interatomic distances. The dominant term of the potential function at large distances is given by the van der Waals interaction, inversely proportional to the sixth power of the independent variable with the constant, determined from theory.[8,9] Proceeding in this way we faced a problem how to match the asymptotic expansion of the potential function with its tabulated numerical values (within the accuracy of their calculation) at a suitable sufficiently large distance and calculate correctly the required sets of bound and metastable states.[10]

*The work was partially supported by the RFBR and MECSS, project number 20-51-44001, the Bogoliubov-Infeld program, the Hulubei-Meshcheryakov program, the RUDN University Program 5-100 and grant of Plenipotentiary of the Republic of Kazakhstan in JINR.

Send correspondence to V.L.D.: E-mail: derbovvl@gmail.com, Telephone: +7 927 220 8353

Saratov Fall Meeting 2020: Laser Physics, Photonic Technologies, and Molecular Modeling, edited by Vladimir L. Derbov, Proc. of SPIE Vol. 11846, 118460Y · © 2021 SPIE
CCC code: 1605-7422/21/$21 · doi: 10.1117/12.2585634

Table 1. Comparison of the vibrational spectra $\tilde{E}_{v=0L=0} - \tilde{E}_{vL=0}$ (in cm^{-1}) for the $X_1\Sigma_g^+$ state of the beryllium dimer: the eigenvalues of vibrational energy $-\tilde{E}_{vL=0}$ (in cm^{-1}) of the beryllium diatomic molecule calculated by the KANTBP 4M[14] and ODPEVP[11] programs implementing FEM (FEM), theoretical (EMO) and experimental (Exp) results,[6] combined ab initio[2] and EMO calculations tabulated as modified EMO (MEMO),[3] symmetry-adapted perturbation theory (SAPT),[1] the Morse-long range (MLR) function and Chebyshev polynomial expansion (CPE)[5] 19 09 2019 and Slater-type orbitals(STO);[4] D_e is the well depth and D_0 is the dissociation energy in cm^{-1}, r_e is the equilibrium internuclear distance in Å, RMS is root-mean-square (RMS) dicrepancy between the theoretical and experimental data.

n	v	FEM	MEMO	EMO	Exp	SAPT	MLR&CPE	STO
	r_e	2.4534	2.4534	2.4535	2.4536	2.443	2.445	2.4344
	D_e	929.804	929.74	929.74	929.7±2	938.7	934.8	934.6±2.5
1	D_0	806.07	806.48	806.5	807.4	812.4	808.1510	807.7
2	1	222.50	222.16	222.7	222.6	222.3	222.9170	223.4
3	2	397.34	397.6	397.8	397.1	397.6	397.4191	400.1
4	3	517.71	517.87	518.2	518.1	520.3	518.4196	517.3
5	4	594.89	595.06	595.4	594.8	597.9	595.0856	595.1
6	5	651.91	652.10	652.4	651.5	655.1	651.7974	651.7
7	6	698.92	699.14	699.4	698.8	702.6	699.0308	698.7
8	7	737.72	737.97	738.2	737.7	741.7	737.9791	738.0
9	8	768.27	768.56	768.8	768.2	772.4	768.5002	769.3
10	9	789.74	790.05	790.7	789.9	794.3	790.1738	790.1
11	10	801.66	802.08	803.4	802.6	807.1	802.8323	802.6
12	11	805.74	806.21			811.9	807.5335	807.5
RMS		0.4	0.4	0.6		3.4	0.3	1.1

In the present paper we continue studying these problems. We recall the results of vibration-rotation bound states and present the improved calculations of the rotation-vibration metastable states of diatomic beryllium molecule having complex-valued eigenenergies. The existence of these metastable states is confirmed by calculation of the corresponding scattering states with real values of resonance energies. High-precision theoretical estimates are of significant importance for further experiments in laser spectroscopy of the diatomic beryllium molecule.

The development of technique for solving the above class of eigenvalue problems for the SOODE using the programs ODPEVP[11] and KANTBP 5M,[12,13] i.e., the upgraded version of KANTBP 4M,[14], implementing the finite element method[15,16] in Fortran and Maple, respectively, is also a subject of the present study.

The paper has the following structure. Section 2 describes the procedure of approximation of potential curve and its extension on large interval by means of the matching procedure using Hermite interpolation polynomials. In Section 3 we present the results of calculating the spectrum of vibration-rotation bound states of the beryllium dimer. Section 4 demonstrates the calculation of beryllium dimer rotation-vibration metastable states with complex values of eigenenergy. In section 5 we present examples of scattering states at resonance energies that confirm the existence of the typical metastable states under consideration. The Appendix presents the Maple subroutine for calculating the potential curve in an extended interval and the input of KANTBP 5M for the calculation of metastable states. In Conclusion we discuss further applications of the elaborated method and results.

2. THE POTENTIAL CURVE AND ITS EXTENSION ON A LARGE INTERVAL

In quantum chemical calculations, the effective potentials of interatomic interaction are presented in the form of numerical tables calculated with limited accuracy and defined on a nonuniform mesh of nodes in a finite domain of interatomic distance variation. However, for a number of diatomic molecules the asymptotic expressions for the effective potentials are calculated analytically for sufficiently large distances between the atoms. The Schrödinger equation for a diatomic molecule in the crude adiabatic approximation, commonly referred to as Born–Oppenheimer (BO) approximation, has the form

$$\left(-\frac{\hbar^2}{2mDa\text{Å}^2}\left(\frac{1}{r^2}\frac{d}{dr}r^2\frac{d}{dr}\right)+\tilde{V}_L(\tilde{r})-(cm^{-1})\tilde{E}_{vL}\right)\tilde{\Phi}_{vL}(\tilde{r})=0, \quad \tilde{V}_L(\tilde{r})=(aue)\tilde{V}(\tilde{r})+\frac{\hbar^2}{2mDa\text{Å}^2}\frac{L(L+1)}{r^2}, \qquad (1)$$

where L is the total angular momentum quantum number, $\hbar^2/(2Da)=1.685762920\cdot10^{-7}$ Å, the reduced mass of beryllium molecule is $m=M/2=4.506$, $\tilde{r}=r$ Å, the effective potential is $\tilde{V}(\tilde{r})$ in atomic units $aue=0.002194746314$

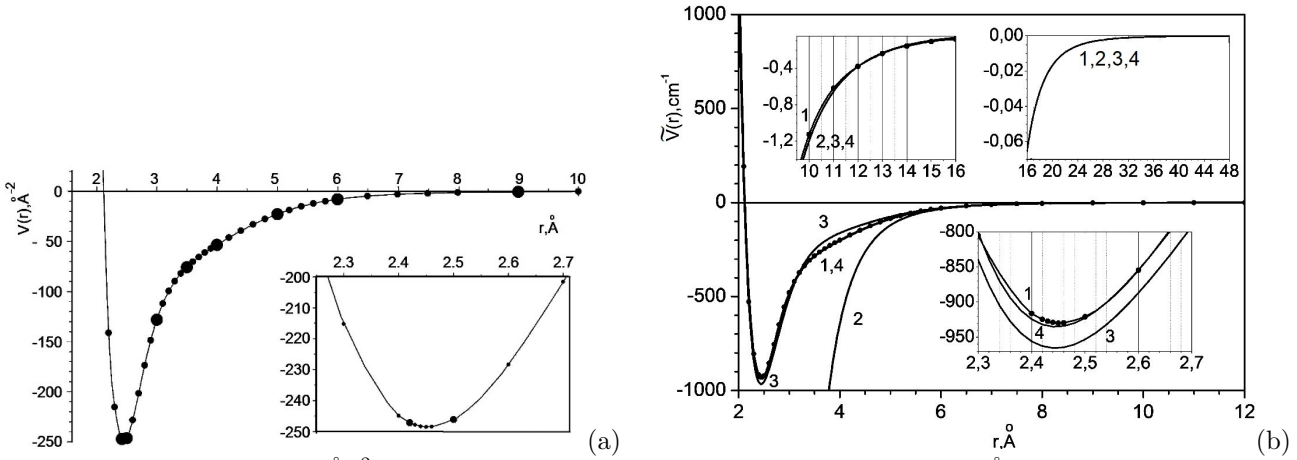

Figure 1. (a) Potential $V(r)$ (Å^{-2}) of the beryllium diatomic molecule as a function of r (Å) obtained by interpolating the tabulated values[3] (points in the subintervals, the boundaries of which are shown by larger-size circles) by fifth-order LIPs. (b) MEMO potential $V(r)$ (points and line 1[3]), the asymptotic expansion $V_{\rm as}(r)$ of MEMO function (line 2,[9]), the analytical forms of the potential function $V_{an}(r)$ (line 3[8] and line 4[5]). r is given in Å, $V_*(r)$ in cm^{-1}.

Å^{-1}, $Da = 9.10938356 \cdot 10^{-31}kg=$ 931.494061MeV is the dalton (atomic mass unit),[17] the energy is $\tilde{E}_{vL}$ cm^{-1}. The BVP for Eq. (1) was solved in the following units: the variable r is expressed in (Å), the effective potential $V(r) = (2mDa\text{Å}^2 aue/\hbar^2)\tilde{V}(r\text{Å})$=58664.99239 $\tilde{V}(r$Å$)$ Å^{-2}, and the desired value of energy E_{vL}=$(2mDa\text{Å}^2/\hbar^2)\tilde{E}_{vL}$ in Å^{-2}, the momentum (wave number) $k = \sqrt{E}$ in Å^{-1} and $\tilde{E}_{vL}$=$s_2 E_{vL}$ cm^{-1}, where $s_2 = 1/0.2672973729$ is the conversion factor from cm^{-1} to Å^{-2}.

In Ref.[3] the potential $\tilde{V}(r)$ (in cm^{-1}) (see Fig. 1) is given by the BO potential function marked as MEMO tabular values $\{\tilde{V}^M(r_i)\}_{i=1}^{76}$ in interval $r \in [r_1 = 1.5, r_{76} = 48]$Å. These tabular values were chosen to provide the best approximation of the potential $\tilde{V}(r)$ by the fifth-order Lagrange interpolation polynomials (LIPs) of the variable r in subintervals $r \in [r_{5k-4}, r_{5k+1}]$, $k = 1, ..., 15$. Indeed, one can see that Fig. 1a displays a smooth approximation till $r_{49} = 12$, where the approximate potential curve coincides with and crosses the asymptotic potential $V_{\rm as}(r)$ given analytically by the expansions[9]

$$V_{\rm as}(r)\text{=}58664.99239\tilde{V}_{\rm as}(r), \quad \tilde{V}_{\rm as}(r)\text{=}-\left(214(3)Z^{-6}\text{+}10230(60)Z^{-8}\text{+}504300Z^{-10}\right), \quad Z = r/0.52917. \qquad (2)$$

This fact allows considering the interval $r \in [r_{\rm match} \geq 12, \infty)$ as possible for using the asymptotic potential $V_{\rm as}(r)$ at large r and executing conventional calculations based on tabular values of $V(r)$ in the finite interval $r \in [r_1, r$=12] (see also[4]). However, the above MEMO tabular values have been calculated in the unusually larger interval $r \in [r_1, r$=48] using special composite basis functions in different subintervals, taking into account both polarization and relativistic corrections DK-MRCI in the subinterval $r \in [r = 12, r = 48]$.[2] We note that the MEMO tabular values for $r \in \{r_{41} = 6.5, ..., r_{48} = 11\}$ are smaller than the asymptotic ones by $5.5 \div 6\%$, for $r = r_{51} = 14$ exceed the asymptotic ones by 8%, and beyond the interval $r \in [r_{40} = 6.0, ..., r_{52} = 15]$ the difference is more than 10%. Based on this fact, in Ref.[10] we considered three cases of approximation of this potential function in the extended interval marked by the key $K = -1$, -3 or -4.

Here we use only the key $K = -1$, the potential $V(r)$ in subintervals $r \in [r_{5k-4}, r_{5k+1}]$, $k = 1, ..., 9$ was approximated by the fifth-order interpolation Lagrange polynomials of the variable r in the interval $r \in [r_1, r_{46} = 14]$. In subinterval $r \in [r_e = r_{46} = 9, r_{\rm match} = 14]$ we consider the approximation of the potential $V(r)$ by the fourth-order interpolation Hermite polynomial using the values of the potential $V(r)$ at the points $r = \{r_e = r_{46} = 9, r_{47} = 10, r_{48} = 11\}$ and the values of the asymptotic potential $V_{\rm as}(r)$ and its derivative $dV_{\rm as}(r)/dr$ at the point $r = r_{\rm match} = 14$. In the $r \in [r_{\rm match} = 14, \infty)$ the potential $V(r)$ is approximated by the asymptotic expansion (2). This approximation has been accepted in our paper.[7]

For comparison we show in Fig. 1 the potential function $\tilde{V}(r)$, its asymptotic expansion $\tilde{V}_{\rm as}(r)$ and the analytical potential functions $\tilde{V}_{an}(r)$ in a.u. (converted into cm^{-1}), proposed in Ref.[8] The MEMO potential function

Table 2. Vibration-rotation bound states $-\tilde{E}_{vL}$ (in cm^{-1}) of beryllium diatomic molecule.

L	v =0	1	2	3	4	5	6	7	8	9	10	11
0	806.07	583.57	408.74	288.37	211.19	154.16	107.15	68.35	37.80	16.33	4.41	0.32
1	804.85	582.44	407.73	287.51	210.48	153.54	106.60	67.87	37.40	16.03	4.21	0.24
2	802.43	580.17	405.70	285.82	209.06	152.31	105.51	66.93	36.61	15.42	3.81	0.095
3	798.78	576.77	402.68	283.27	206.94	150.46	103.89	65.51	35.42	14.51	3.23	
4	793.93	572.24	398.64	279.88	204.11	148.00	101.72	63.63	33.84	13.31	2.48	
5	787.86	566.58	393.61	275.66	200.59	144.93	99.02	61.28	31.89	11.83	1.57	
6	780.59	559.79	387.57	270.60	196.38	141.27	95.79	58.48	29.56	10.09	0.56	
7	772.11	551.88	380.55	264.73	191.49	137.01	92.04	55.24	26.88	8.11		
8	762.43	542.85	372.54	258.04	185.93	132.16	87.79	51.56	23.85	5.91		
9	751.55	532.71	363.56	250.56	179.71	126.74	83.03	47.47	20.50	3.54		
10	739.47	521.45	353.60	242.29	172.84	120.76	77.78	42.96	16.84	1.02		
11	726.20	509.10	342.69	233.26	165.34	114.22	72.06	38.06	12.92			
12	711.74	495.65	330.84	223.48	157.23	107.15	65.88	32.80	8.75			
13	696.09	481.12	318.05	212.98	148.51	99.55	59.25	27.18	4.40			
14	679.27	465.50	304.35	201.77	139.21	91.45	52.20	21.25				
15	661.28	448.81	289.75	189.88	129.36	82.86	44.76	15.04				
16	642.12	431.07	274.28	177.35	118.97	73.81	36.94	8.59				
17	621.80	412.27	257.94	164.21	108.06	64.32	28.78	*1.95				
18	600.34	392.44	240.78	150.49	96.67	54.42	20.31					
19	577.72	371.59	222.81	136.25	84.82	44.14	11.59					
20	553.98	349.73	204.07	121.52	72.53	33.51	*2.66					
21	529.10	326.87	184.61	106.35	59.85	22.58						
22	503.11	303.05	164.46	90.81	46.82	11.40						
23	476.02	278.27	143.68	74.95	33.46	*0.017						
24	447.82	252.56	122.33	58.84	19.83							
25	418.55	225.94	100.49	42.53	*5.98							
26	388.20	198.45	78.27	26.09								
27	356.79	170.11	55.77	9.58								
28	324.34	140.96	33.18									
29	290.86	111.05	10.70									
30	256.36	80.42										
31	220.87	49.14										
32	184.41	17.28										
33	146.98											
34	108.63											
35	69.36											
36	29.21											

$\tilde{V}(r)$ is seen to have a minimum $-D_e(\mathrm{FEM})=\tilde{V}(R_e)=-929.804\mathrm{cm}^{-1}$ at the equilibrium point R_e=2.4534 Å and shifts above the analytical potential function $\tilde{V}_{\mathrm{an}}(r)$ in the vicinity of this point $-D_e(\mathrm{Sheng})=\tilde{V}_{\mathrm{an}}(R_e)=-948.3\mathrm{cm}^{-1}$, while the analytical potential function $\tilde{V}_{\mathrm{an}}(r)$ lies above the MEMO potential function $\tilde{V}(r)$ in the interval $r\in(3.2, 6.1)$. Thus, using the accepted approximation with the key $K=-1$ we have the potential function $\tilde{V}(r)$ in the analytical form in interval $r\in(1.9, 14)$ and its smooth continuation at $r \geq 14$ by means of the asymptotic expression (2).

3. BOUND STATES

The BVP for Eq. (1) was solved using the FEM programs KANTBP 4M and ODPEVP on the finite element mesh

$$\Omega_1 = \{1.90, 1.95, 2.00, 2.07, 2.15, 2.22, 2.30, 2.36, 2.42, 2.50(0.1)4(0.2)6(0.5)14(2)44\} \tag{3}$$

with the second-type or Neumann boundary conditions (BCs) on the boundary points of the mesh. In each of the subintervals (except the last one) the potential $V(r)$ was approximated by a LIP of the fifth order. In Appendix we present the function $V(r)$ in $\mathrm{Å}^{-2}$, the values of r in Å, and the input file for calculating eigenvalues, S-matrix, and corresponding wave functions of bound, metastable and scattering states by means of KANTBP 5M program. In the BVP solution at all finite elements of the mesh the local functions were represented by fifth-order HIPs.

Table 1 presents the results of using FEM programs KANTBP 4M and ODPEVP to calculate 12 eigenvalues of beryllium diatomic molecule. It shows the eigenvalues calculated with the ab initio modified expanded Morse oscillator (MEMO) potential function[3] and the corresponding FEM approximation. In contrast to the original EMO function, which was used to describe the experimental (Exp) vibrational levels,[6] it has not only the correct dissociation energy, but also describes all twelve vibrational energy levels with the RMS error less than 0.4 cm^{-1}.

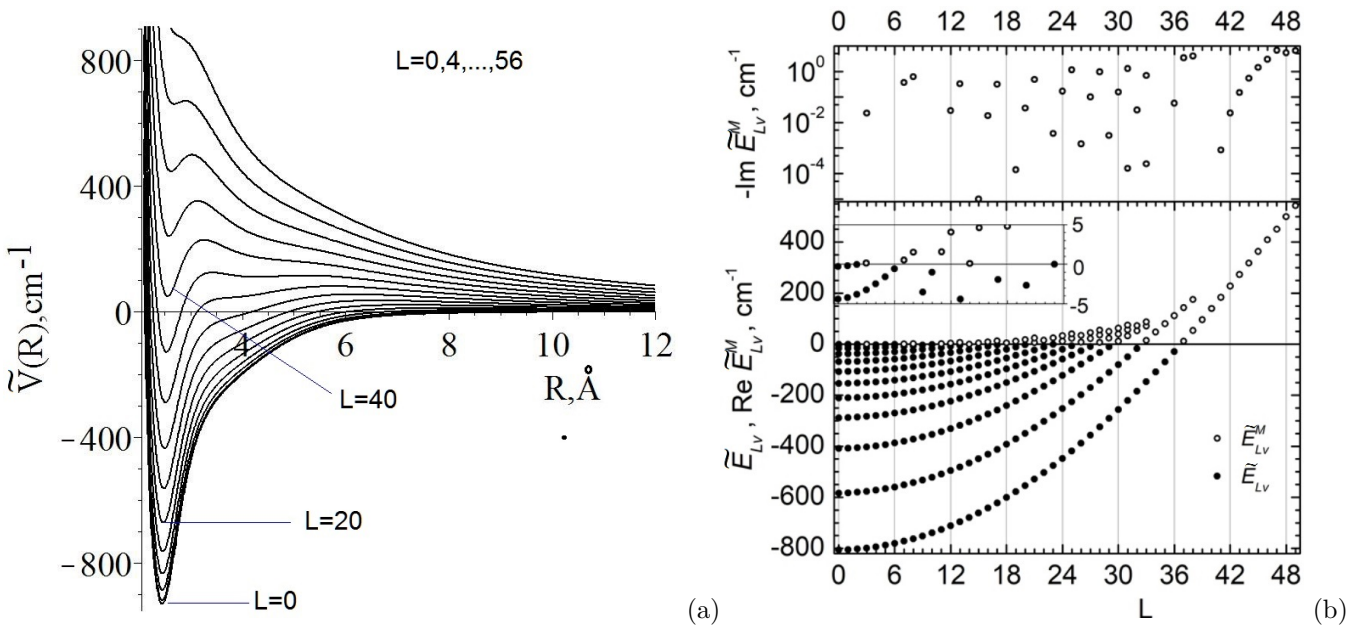

Figure 2. (a) Potential functions $V_L(r)$ at $L = 0, 4, 8, ..., 56$. (b) Eigenenergies E_{vL} of vibration-rotation bound states (lower panel) and real part $\Re E^M_{Lv}$ (lower panel) and imaginary part $-\Im E^M_{Lv}$ with negative sign (upper panel) of complex eigenenergies $E^M_{Lv} = \Re E^M_{Lv} + i\Im E^M_{Lv}$ of rotation-vibration metastable states. The potential functions $V_L(r)$ at $L = 0, 1, ..., 36$ and at $L = 0, 4, 8, ..., 56$. Note that the bound states are supported by the potentials $V_L(r)$ at $L = 0, 1, ..., 36$ (see Table 2 and Fig. 2 a), while the metastable states are supported by the potentials $V_L(r)$ at $L = 3, 7, 8, 11, 12, 14, 15, 16, 18, 19, 20, 21, 22, 23, 24, 25, 26, 27, 28, 29, 30, 31, 32, 33, 34, 35, 36, 37, 38, 39, 40, 41, 42, 43, 44, 45, 46, 47, 48, 49$ (see Table 3 and Fig. 2 a)

The table also shows the results of recent calculation using the Morse long-range (MLR) function and Chebyshev polynomial expansion (CPE) alongside with the EMO potential function.[5] Similar results were obtained by Lesiuk et al.[4] The main attention in the optimization of the MLR and CPE functions was focused on their correct long-range behavior displayed in Fig. 1. However, there are some problems with the quality of the MLR and CPE potential curves.[3] As a consequence, one can see from the table, that the corresponding results provide *a lower estimate* whereas FEM and MEMO results give *an upper estimate* for the discrete spectrum of the diatomic beryllium molecule.

The potential functions $\tilde{V}_L(r)$ from $L = 0$ to $L = 36$ support $37+33+30+28+26+24+21+18+14+11+7+3 = 252$ vibration-rotation levels $-\tilde{E}_{vL}$ presented in Table 2. Note that four states marked by asterisk in Table 2 are added as a result of applying a denser finite-element mesh (3). Figure 2b shows also the rotation-vibration spectrum $\tilde{E}_{vL} \equiv \tilde{E}_{vL}$ (in cm^{-1}) of Be_2 vs L. These functions $\tilde{V}_L(r)$ are displayed in Fig. 2a at $L = 0, ..., 36$ with the step 4. One can see that the potential $V_L(r)$ at $L = 0$, $L = 1$ and $L = 2$ supports 12 vibrational energy levels.

4. METASTABLE STATES

The complex eigenenergies $\tilde{E}^M_{Lv} = \Re\tilde{E}^M_{Lv} + i\Im\tilde{E}^M_{Lv}$, (in cm^{-1}) of Be_2 rotation-vibration metastable states, where v is the number of states at fixed value of L, are shown in Table 3. Their real parts $\Re E^M_{Lv}$ in comparison with the eigenenergies $\tilde{E}_{vL}$ of vibration-rotation bound states are displayed in lower panel of Fig. 2b. Note that the real parts of energies $\Re E^M_{Lv}$ of the metastable states marked by an asterisk in Table 3 lie above the top $V^{\max}_L$ of the potential barrier $V_L(r)$. The BVP for Eq. (1) was solved by the FEM programs on the above finite element mesh Ω_1 with mixed BVPs, i.e. the Neumann BC at the left point r_1 of the finite interval $r \in [r_1, r^{\max}]$ and the third-type or Robin BC at the right point r_{max} which is calculated using the corresponding asymptotic solution $\Phi^{M(\mathrm{as})}_{Ln}(r)$ in the form of an outgoing wave.[16]

Table 3. The rotation-vibration metastable states $\tilde{E}^M_{Lv} = \Re\tilde{E}^M_{Lv} + \Im\tilde{E}^M_{Lv}$ (in cm^{-1}) of Be_2, where "eps" means that $-10^{-5} < \Im\tilde{E}^M_{Lv} < 0$ (in cm^{-1}).

L	v	$V_L^{\min}$	$V_L^{\max}$	$\Re E$	$-\Im E$
0		-929.74	0.00		
1		-928.49	0.01		
2		-926.00	0.04		
3	11	-922.26	0.12	0.092	0.014
4		-917.27	0.22		
5		-911.04	0.42		
6		-903.59	0.71		
7	10	-894.94	1.11	0.504	5.5e-4
8	10	-885.05	1.62	1.508	0.078
9		-873.92	2.24		
10		-861.56	3.00		
11	9	-847.96	3.92	1.554	eps
12	9	-833.12	5.02	4.050	0.031
13		-817.04	6.27		
14	8	-799.73	7.73	0.083	eps
15	8	-781.19	9.39	4.605	1.e-5
16	8	-761.44	11.26	8.992	0.018
17	8	-740.59	13.34	13.016	0.314
18	7	-718.51	15.66	4.788	eps
19	7	-695.21	18.22	11.517	1.4e-4
20	6	-670.68	21.05	17.991	0.036
21	6	-644.93	24.15	6.403	eps
21	7	-644.93	24.15	23.915	0.482
22	6	-618.07	27.51	15.497	eps
23	5	-590.08	31.24	24.444	3.7e-3
24	5	-561.68	35.18	11.484	eps
24	6	-561.68	35.18	32.872	0.169
25	4	-531.76	39.58	22.998	eps
*25	5	-531.76	39.58	40.608	1.156
26	4	-500.63	44.18	7.996	eps
26	5	-500.63	44.18	34.354	1.4e-3
27	4	-468.31	49.30	22.032	eps
27	5	-468.31	49.30	45.187	0.100
28	3	-434.78	54.66	6.963	eps
28	4	-434.78	54.66	35.991	eps
*28	5	-434.78	54.66	55.158	0.963
29	3	-400.25	60.57	23.517	eps
29	4	-400.25	60.57	49.669	3.0e-4
30	2	-364.62	66.91	11.354	eps
30	3	-364.62	66.91	40.058	eps
30	4	-364.62	66.91	62.639	0.155
31	2	-327.81	73.60	32.621	eps
31	3	-327.81	73.60	56.534	1.6e-4
*31	4	-327.81	73.60	74.625	1.305
32	2	-290.09	80.68	52.660	eps
32	3	-290.09	80.68	72.662	0.030
33	1	-251.21	88.21	15.028	eps
33	2	-251.21	88.21	71.131	2.4e-4
33	3	-251.21	88.21	87.630	0.696
34	1	-211.33	80.42	47.644	eps
35	1	-170.41	101.47	80.254	eps
36	1	-128.47	124.02	111.593	0.057
37	0	-85.56	147.94	11.780	eps
37	1	-85.56	147.94	143.263	3.429
38	0	-41.66	173.18	53.590	eps
*38	1	-41.66	173.18	174.945	4.014
39	0	3.20	199.73	96.169	eps
40	0	48.96	227.57	139.466	eps
41	0	95.70	256.70	183.406	8.3e-4
42	0	143.28	287.15	227.880	0.023
43	0	191.72	318.91	272.755	0.148
44	0	241.02	352.03	317.922	0.544
45	0	291.13	386.52	363.371	1.432
46	0	342.01	422.41	409.200	3.007
47	0	393.59	459.74	450.402	6.810
*48	0	445.84	498.57	499.563	5.439
*49	0	498.71	538.92	542.927	6.046
50		552.15	580.82		
51		606.00	624.52		
52		660.18	670.09		
53		714.45	717.43		
54					

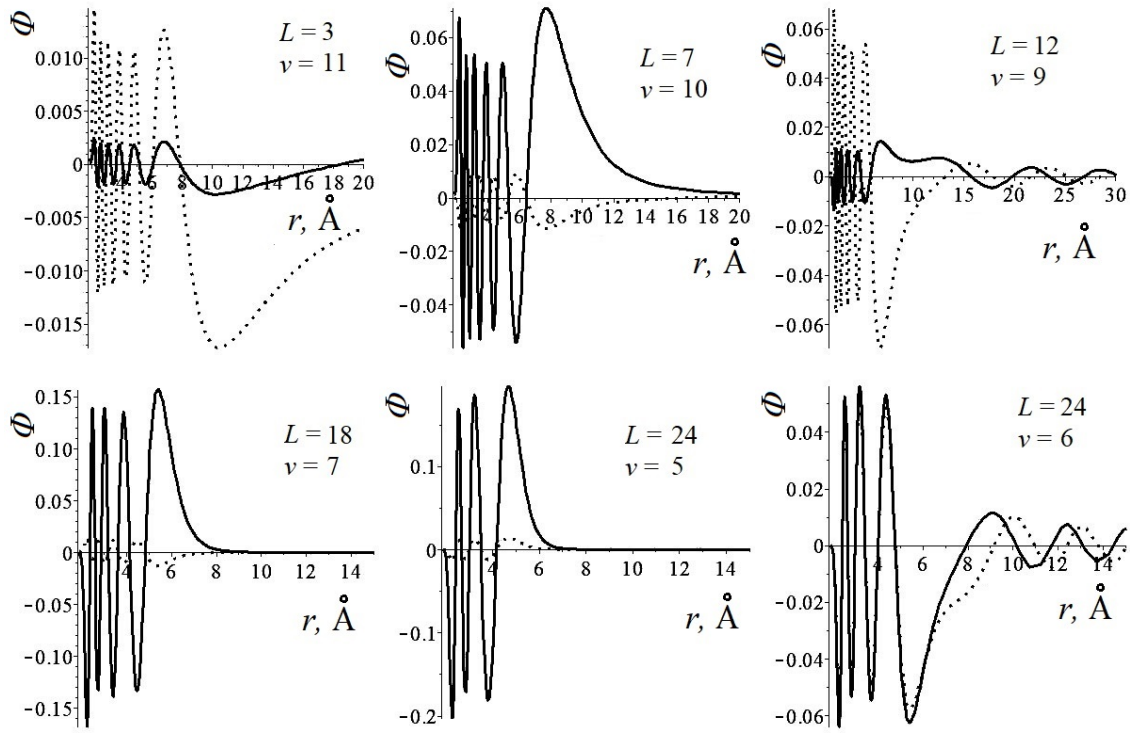

Figure 3. Plots of real (solid curve) and imaginary (dashed curve) parts of eigenfunctions $\Phi^M_{Lv}(r)$ of selected metastable states having eigenvalues from the table marked by $L = 3, 7, 12, 18, 24$ and v.

The BVP for Eq. (1) was solved using the FEM programs KANTBP 5M on the finite element mesh

$$\Omega_1 = \{1.90, 1.95, 2.00, 2.07, 2.15, 2.22, 2.30, 2.36, 2.42, 2.50(0.1)4(\gamma_1)6(\gamma_2)14(\gamma_3)\gamma_4\},$$

where $\gamma_1 = \{0.2, L < 44; 0.1\}$, $\gamma_2 = \{0.5, L < 25; 0.25, L < 38; 0.1(6), L < 44; 0.125\}$, $\gamma_3 = 3.1/\sqrt{V^{\max}_{L_9}}$, $L_9 = \max(L, 9)$ γ_4 is the lowest number of sequence $14 + k\gamma_3$, $k \in \mathcal{N}$ greater than 80, with the Neumann boundary conditions (BCs) on the boundary point $r = 1.90$ and the Robin boundary condition with logarithmic derivative

$$\frac{d\Phi(kr)}{dr} - R\Phi(kr) = 0, \quad R = \frac{1}{\Phi^+_{as}(kr)}\frac{d\Phi^+_{as}(kr)}{dr} = \frac{L}{r} - k\frac{H^{(1)}_{L+3/2}(kr)}{H^{(1)}_{L+1/2}(kr)}, \quad k = \sqrt{E} = \sqrt{\frac{\tilde{E}}{s_2}} \tag{4}$$

$$\Phi^{\pm}_{as}(kr) = \frac{\sqrt{\pi/2}}{\sqrt{r}}H^{(1,2)}_{L+1/2}(kr) = \mp\imath\frac{\exp(\pm\imath(kr - \pi L/2))}{\sqrt{kr}} + O(k^{-3/2}r^{-2})$$

that followed from asymptotic solution. where E given in cm^{-1}, $H^{(1,2)}_{L+1/2}(r)$, $H^{(1,2)}_{L+3/2}(r)$ are Hankel functions ($\frac{d}{dz}H^{(1,2)}_{L+1/2}(z) = (L+1/2)H^{(1,2)}_{L+1/2}(z)/z - H^{(1)}_{L+3/2}(z)$) and $s_2 = 1/0.2672973729$ is the conversion factor from cm^{-1} to $\mathring{A}^{-2}$. The potential functions $V_L(r)$ at $L = 3, 7, 8, 11, 12, 14, ..., 49$ supported this set of metastable states. These functions are plotted in Fig. 2a at $L = 8, ..., 56$ with the step 4. For $L > 0$ the potential functions at large r decrease proportionally to r^{-2} and at $L \le 38$ have the form of a potential well with a minimum below the dissociation threshold D_0, while at $L > 38$ the potential well has a minimum above the dissociation threshold. The height of the centrifugal barrier increases with increasing L, but its width at the dissociation threshold energy is infinite. With increasing energy, the effective width of the barrier decreases. The number of metastable states δv at $L \le 38$ is determined by the number of positive-energy states in the potential well with the barrier with the height $V^{\max}_L$ taken into account, i.e., in the well with the potential $V^*_L = \{V(r), r < r_{\max}; V_{\max}, r \ge r_{\max}\}$.

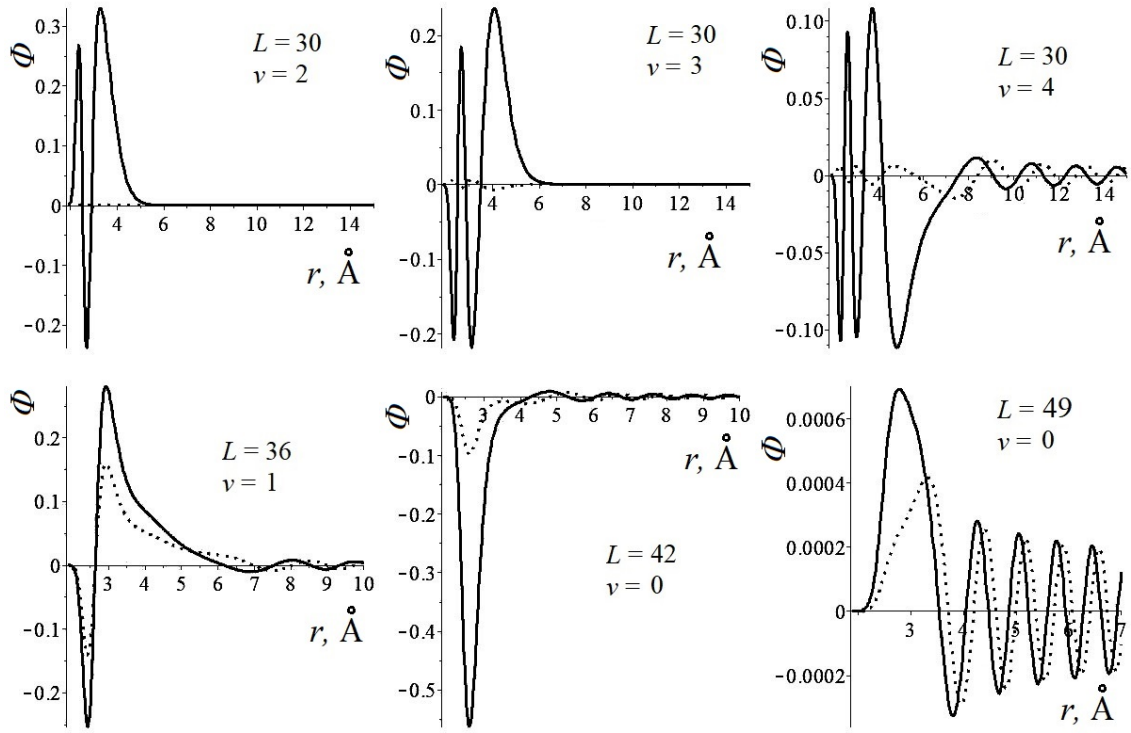

Figure 4. Plots of real (solid curve) and imaginary (dashed curve) parts of eigenfunctions $\Phi^M_{Lv}(r)$ of selected metastable states having eigenvalues from the table marked by $L = 30, 36, 42, 49$ and v.

For small $L < 16$ the barrier height $V_L^{\max}$ counted from the zero energy is smaller than the energy difference between two upper levels of metastable states. This means that even one metastable state can exist not for all values of L. With the growth of L to $L = 33$ the barrier height increases, but the width of the well changes insignificantly. As a result, the number of metastable states increases to three. With further increase in L, when in the interval $r \in (3.5, 6)$ the slope of centrifugal potential exceeds the slope of MEMO potential, the well width rapidly decreases, so that only two states can exist in the well, a bound state and a metastable one at $L = 34, 35, 36$ and two metastable states at $L = 37, 38$. At $L \geq 39$ the potential well minimum turns to be above the dissociation threshold and the effective barrier width, the width and depth of the well decrease. Only one state exists in the well, its width increasing with the growth of L. At $L > 49$ there are no energy levels in the well, and at $L > 54$ the potential well disappears.

As can be seen from Tables 2 and 3 and Figures 3–4, the eigenfunctions of metastable states with complex energy values for a fixed value of the orbital momentum L have an increasing number of nodes localized inside the potential well. Beginning from each lower state above the dissociation threshold, they have has one node more than the last bound state with real energy under the dissociation threshold ($E = 0$) with the same value of the orbital momentum L. Thus, there is a continuation of the real energy eigenvalues $\tilde{E}_{Lv} = \Re\tilde{E}_{Lv}$ to the complex plane $\tilde{E}^M_{Lv} = \Re\tilde{E}^M_{Lv} + \imath\Im\tilde{E}^M_{Lv}$, labelled by the number of nodes of eigenfunctions localized inside the potential well, for each value of the orbital moment L.

5. SCATTERING STATES

The scattering problem for Eq. (1) was solved using the FEM programs KANTBP 5M on the finite element mesh

$$\Omega_1 = \{1.90, 1.95, 2.00, 2.07, 2.15, 2.22, 2.30, 2.36, 2.42, 2.50(0.1)4(\gamma_1)6(\gamma_2)14(\gamma_3)\gamma_4\},$$

where $\gamma_1 = \{0.2, \tilde{E} < 360; 0.1\}$, $\gamma_2 = \{0.5, \tilde{E} < 35; 0.25, \tilde{E} < 1488; 0.1(6), \tilde{E} < 320; 0.125\}$, $\gamma_3 = 2.9/\sqrt{\tilde{E}}$, γ_4 is the lowest number of sequence $14 + k\gamma_3$, $k \in \mathcal{N}$ greater than 80. The Robin boundary condition 4 for

eigenfunction of scattering states is formulated using the asymptotic form "incident wave + outgoing wave":

$$\Psi_{as}^{L}(r) = \frac{1}{2}(\Psi_{as}^{-}(kr) + \Psi_{as}^{+}(kr)S_L(E)), \tag{5}$$

where $S_L(E) = \exp(2i\delta_L(E))$ is the partial scattering matrix and $h_L^{(\pm)}(pr)$ are spherical Hankel functions.[18]

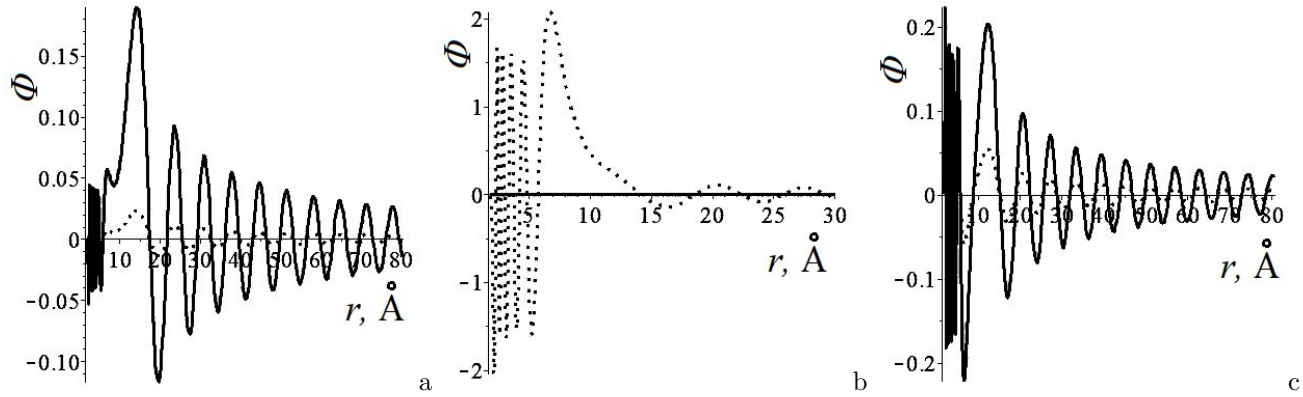

Figure 5. Plots of the real (solid) and imaginary (dashed) parts of scattering functions $\Phi_L(r)$ in the vicinity of the resonance energy $E(res) \approx 4.0444958\text{cm}^{-1}$ at $L = 12$ (b) and at energies $E = E(res) - 0.5\text{cm}^{-1}$ (a) and $E = E(res) + 0.5\text{cm}^{-1}$ (c)

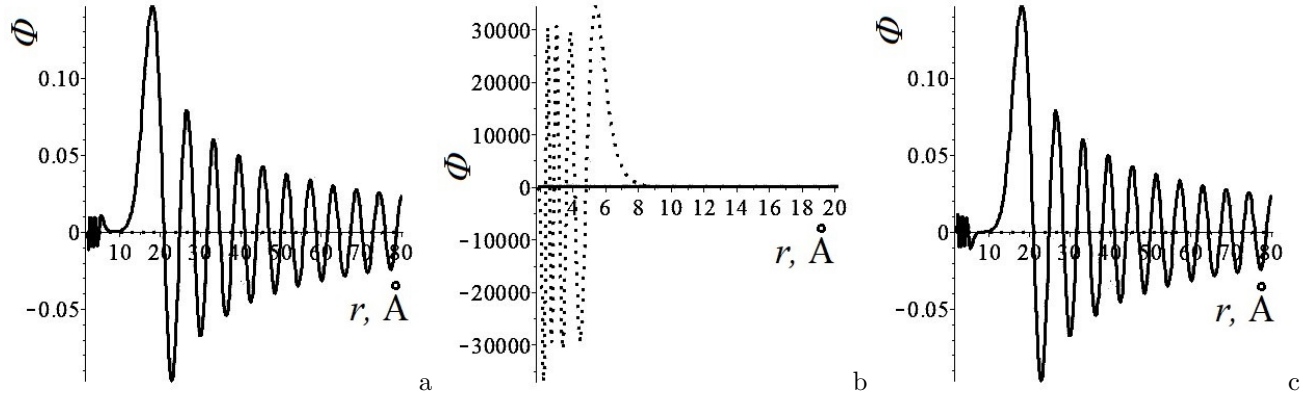

Figure 6. Plots of the real (solid) and imaginary (dashed) parts of scattering functions $\Phi_L(r)$ in the vicinity of resonance energy $E(res) \approx 4.78829358850231\text{cm}^{-1}$ at $L = 18$ (b) and at energies $E = E(res) - 10^{-3}\text{cm}^{-1}$ (a) and $E = E(res) + 10^{-3}\text{cm}^{-1}$ (c)

Plots of the real (solid) and imaginary (dashed) parts of scattering functions in the vicinity of the resonance energy for the narrow resonance at $L = 12$ and very narrow resonance at $L = 18$ are shown in Figs. 5 and 6. One can see that the resonant scattering functions are localized in the potential well, which is no longer observed with a minor change in the energy of the incident wave. As can be seen from Table 3, the energies of resonant states coincide with the real parts of the energies of metastable states. In Fig. 7 the phase shifts δ vs the scattering energy E are shown, as expected, the phase shifts takes the value $\delta = \pi/2$ for resonant energies and change rapidly in their vicinity. In Fig. 8 the wave functions of broad resonance states at $L = 25$ and $L = 49$ are presented. Comparing Fig. 8 and Fig. 4 for $L = 49$ one can see that the wave functions in the potential well infinity also almost coincide up to the phase, but the energies of broad resonance states differ from the real parts of the energies of metastable states.

For rough estimation of scattering length a_S of the scattering state at $k \to 0$ one can apply the formula

$$a_S = -\lim_{k\to 0}\frac{\tan\delta_0(k)}{k} \approx -\left.\frac{d\delta_0(k)}{dk}\right|_{k\to 0} \approx -\left.\frac{\delta_0(k_{i+1}) - \delta_0(k_{i-1})}{k_{i+1} - k_{i-1}}\right|_{k_i\to 0},$$

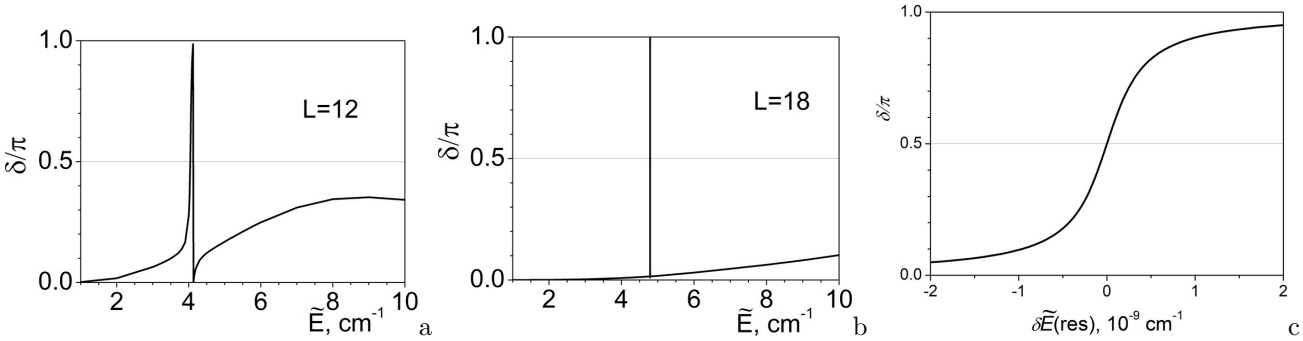

Figure 7. Phase shifts δ vs scattering energy E counted from $E(0)$ at $L = 12$ (a) and $L = 18$ (b). Phase shifts δ at $L = 18$ in the vicinity of resonance energy $E(res)$ (c). Here $\delta E(res) = E - E(res)$.

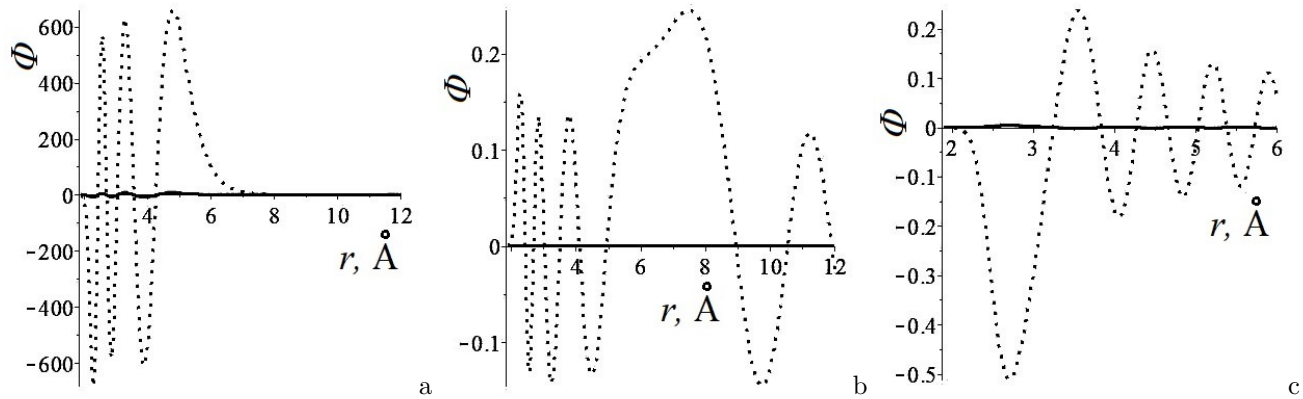

Figure 8. Plots of the real (solid) and imaginary (dashed) parts of scattering functions in the vicinity of resonance energies $E_1(res) = 22.9981893$ and $E_2(res) = 38.684375$ at $L = 25$ (a,b) and $E_1(res) = 562$ at $L = 49$ (c)

where $k^{-1} = \sqrt{\hbar^2/(2\mu E)}$ in $\mathring{A}$ and E in $\mathring{A}^{-2}$ are accepted in our calculations. The calculated plot $-\frac{d\delta_0(k)}{dk} \approx a_S$ presented in Fig.9 gives us an estimate for $a_S \approx 3.348$ Å. For example, a plot of the corresponding wave function is shown at $k = 0.001$.

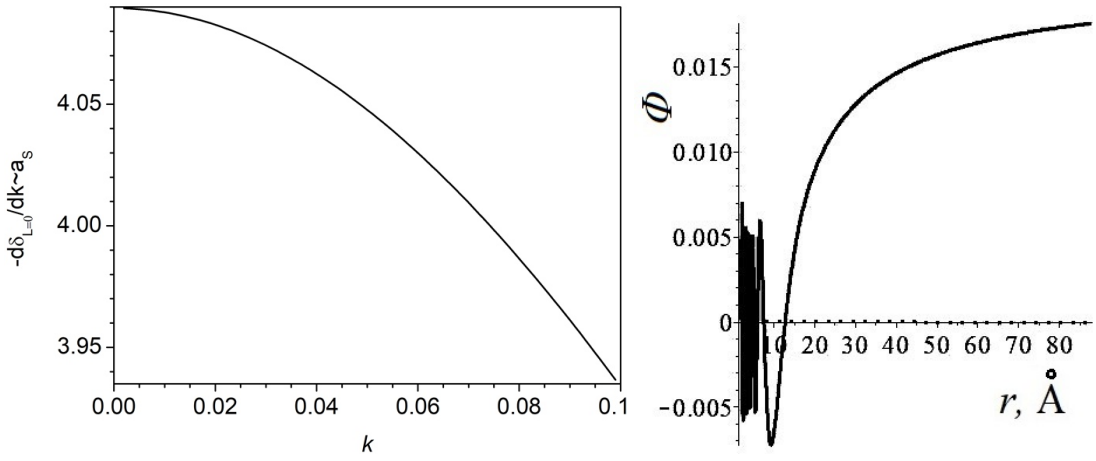

Figure 9. Estimate of scattering length a_S in $\mathring{A}$ vs $k = \sqrt{E}$ in $\mathring{A}^{-1}$ and wave function at $k = 0.001$, $L = 0$.

6. CONCLUSION

The efficacy of the applied programs is demonstrated by the calculations of twelve eigenenergies of the vibrational bound states of the diatomic beryllium molecule with the required accuracy in comparison with those known from literature, as well as the vibration-rotation spectrum bound states and rotation-vibration spectrum of narrow-band metastable states with complex valued eigenenergies. We believe that these results can serve as a guide for future high-precision laser spectroscopy of weakly-bound, metastable and scattering states of the diatomic beryllium molecule. Laser spectroscopy of such objects offers unique opportunities for clarifying the nature of electron correlation bonding in molecules that could not exist in the standard chemical bond theory based on the Hartree-Fock self-consistent field approximation.

The presented approach and KANTBP 5M program[12,13] provide a useful tool for further study of approximations of the tabulated potential function in a finite interval and its extension beyond this interval using asymptotic expansions and its matching via interpolation Hermite polynomials, and modeling calculations of the weakly bound states with eigenenergies close to the dissociation threshold.

APPENDIX A. PROGRAM APPR100(Z,NDIFF) FOR CALCULATION OF THE FUNCTION AND THEIR DERIVATIVES IN MAPLE

This program is generated by KANTBP 5M as file "ap100proc.dat" and formatted by authors to save space.

```
IHPord100:=5;
APPRa100(1):=Array(0..5, [6563.481440,-25773.71080,37646.63813,-21410.9884,-6655.7025,11630.1485]);
APPRa100(2):=Array(0..5, [359.3721451,-3104.297326,-5215.0147,70890.050,-178091.889,145901.634]);
APPRa100(3):=Array(0..5, [-247.1310696,-87.46223573,1940.24795,-37266.546,767534.90,-5122429.0]);
APPRa100(4):=Array(0..5, [-246.1380760,95.5486417,1039.161533,-2399.49691,2045.3678,-559.7915.]);
APPRa100(5):=Array(0..5, [-128.1684292,181.6804438,-224.971337,154.52760,-2.64361,-42.13789]);
APPRa100(6):=Array(0..5, [-75.73714115,58.2170614,-47.294042,60.28050,-47.22552,16.29992]);
APPRa100(7):=Array(0..5, [-53.35927103,37.54337408,-6.7217519,2.0653728,-3.909147,1.5793407]);
APPRa100(8):=Array(0..5, [-22.80208992,22.47494218,-8.23297389,-1.1391093,3.4655190,-1.7463266]);
APPRa100(9):=Array(0..5, [-7.980042026,8.254463698,-4.495464799,1.525957870,-.3023317676,.2625548403e-1]);
APPRa100(10):=Array(0..5, [-.5837591267,.3903170743,-.1264023888,.2045626914e-1,-.1286537989e-2,0]);
APPR100:=proc(z,ndiff)local nelemd,zelemd,EIGFt,IHPordt,j1,j2,res,jc;
jc:=1;
if z < 1.50 or z >  14.
then RETURN(0)
else if z < (3.50)
then if z < (2.42)
then if z < (2.00)
then nelemd:=1; zelemd:=z-(1.50);
else nelemd:=2; zelemd:=z-(2.00); fi;
else if z < (2.50)
then nelemd:=3;zelemd:=z-(2.42);
else if z < (3.00)
then nelemd:=4; zelemd:=z-(2.50);
else nelemd:=5; zelemd:=z-(3.00); fi;fi;fi;
else if z < (5.00)
then if z < (4.00)
then nelemd:=6; zelemd:=z-(3.50);
else nelemd:=7; zelemd:=z-(4.00); fi;
else if z < (6.00)
then nelemd:=8; zelemd:=z-(5.00);
else if z < (9.00)
then nelemd:=9; zelemd:=z-(6.00);
else nelemd:=10; zelemd:=z-(9.00);fi;fi;fi;fi;fi;
EIGFt:=APPRa100(nelemd); IHPordt:=IHPord100;
for j1 from 1 to ndiff do
IHPordt:=IHPordt-1;
for j2 from 0 to IHPordt do EIGFt[j2]:=EIGFt[j2+1]*(j2+1); od;
EIGFt[IHPordt+1]:=0; od;
res:=0; for j2 from 0 to IHPordt do res:=res+EIGFt[j2]*zelemd^j2; od;
RETURN(res);
end;
```

APPENDIX B. INPUT FOR KANTBP 5M IN MAPLE

1. Preparation the coefficients of ODEs (common block)

```
restart;read "kantbp4m.mwt";nexec:=100;keypot:=0;pmax:=5;zmax:=14;
sc1:=58664.99239;sc2:=1/0.2672973729;sc3:=0.52917;
vpotas:=proc(z) -sc1*(214/z^6+10230/z^8+504300/z^10); end;
dvpotas:=proc(z) sc1*(6*214/z^7+8*10230/z^9+10*504300/z^11); end;
fgrid:=[[ 1.50,0.1118807175059 ],[ 1.60,0.0739898922057 ],[ 1.70,0.0466443312944 ],[ 1.80,0.0275431523429 ]
,[ 1.90,0.0145889788722 ],[ 2.00,0.0061258363891 ],[ 2.10,0.0008750047040 ],[ 2.20,-0.0024073301631 ]
,[ 2.30,-0.0036689744392 ],[ 2.40,-0.0041746459684 ],[ 2.42,-0.0042125816352 ],[ 2.43,-0.0042246962019 ]
,[ 2.44,-0.0042324378496 ],[ 2.45,-0.0042362178362 ],[ 2.46,-0.0042354030082 ],[ 2.50,-0.0041956551263 ]
,[ 2.60,-0.0038931591836 ],[ 2.70,-0.0034358549158 ],[ 2.80,-0.0029579508571 ],[ 2.90,-0.0025328802176 ]
,[ 3.00,-0.0021847514842 ],[ 3.10,-0.0019107861711 ],[ 3.20,-0.0016979919870 ],[ 3.30,-0.0015318041849 ]
,[ 3.40,-0.0013994900523 ],[ 3.50,-0.0012910108407 ],[ 3.60,-0.0011988862767 ],[ 3.70,-0.0011177635545 ]
,[ 3.80,-0.0010439586802 ],[ 3.90,-0.0009750528419 ],[ 4.00,-0.0009095589866 ],[ 4.20,-0.0007859660563 ]
,[ 4.40,-0.0006710837021 ],[ 4.60,-0.0005657679843 ],[ 4.80,-0.0004713661945 ],[ 5.00,-0.0003886830799 ]
,[ 5.20,-0.0003177456704 ],[ 5.40,-0.0002579299264 ],[ 5.60,-0.0002081941213 ],[ 5.80,-0.000167514292722]
,[ 6.00,-0.000136027325687],[ 6.50,-0.000081888817926],[ 7.00,-0.000050646242390],[ 7.50,-0.000032288610141]
,[ 8.00,-0.000021178605693],[ 9.00,-0.000009950723641],[10.00,-0.000005125283373],[11.00,-0.000002823983793]];
fgrid:=[seq([fgrid[i,1],sc1*fgrid[i,2]],i=1..nops(fgrid)),[zmax,vpotas(zmax/sc3),dvpotas(zmax/sc3)/sc3]];
hermites();
IHPtype:=[3,3];
fa:=proc(z) z^2*sc2; end;
fb:=proc(z) z^2; end;
read "ap100proc.dat":
vpot:=proc(z)(`if`(z<zmax,APPR100(z,0),vpotas(z/sc3))+L*(L+1)/z^2)*sc2; end;
```

2. Solution of the bound states problem

```
Emax:=0.0;keypot:=1;L:=0;
zmesh:=[1.90,1.95,2.00,2.07,2.15,2.22,2.30,2.36,2.42,seq(2.50+0.1*i,i=0..14),seq(4.00+0.2*i,i=0..9)
,seq(6.00+0.5*i,i=0..15),seq(14.00+2.*i,i=0..15)];

hermites();
```

3. Solution of the scattering problem

```
RBC:=proc(Rp2OC,RBoundLR,RBoundRL,DRBoundLR,DRBoundRL,RBoundC,DRBoundC) local HHC,HH1,HH2,HHH1,HHH2;
  Rp2OC[1]:=Eh/sc2;
  HHC:=evalf(sqrt(Pi/2)/sqrt(zmesh[-1]));
  HH1:=HankelH1(L+1/2,sqrt(Rp2OC[1])*zmesh[-1]);
  HH2:=HankelH2(L+1/2,sqrt(Rp2OC[1])*zmesh[-1]);
  HHH1:=HankelH1(L+3/2,sqrt(Rp2OC[1])*zmesh[-1]);
  HHH2:=HankelH2(L+3/2,sqrt(Rp2OC[1])*zmesh[-1]);
  RBoundLR[1,1] :=evalf(HHC*HH1);
  RBoundRL[1,1] :=evalf(HHC*HH2);
  DRBoundLR[1,1]:=evalf(HHC*(L*HH1/(zmesh[-1])-HHH1*sqrt(Rp2OC[1])));
  DRBoundRL[1,1]:=evalf(HHC*(L*HH2/(zmesh[-1])-HHH2*sqrt(Rp2OC[1])));
  RBoundC[1,1]  :=0;
  DRBoundC[1,1] :=0;

RETURN();
end;

keypot:=2;DirL:=2;DirR:=-1;L:=25;Eh:=22.9981893;
zmesh:=[1.90,1.95,2.00,2.07,2.15,2.22,2.30,2.36,2.42,seq(2.50+0.1*i,i=0..14)
  ,`if`(Eh>360.,seq(4.00+0.1*i,i=0..19),seq(4.00+0.2*i,i=0..9))
   ,`if`(Eh<35.,seq(6.00+0.5*i,i=0..15)  ,`if`(Eh<148.,seq(6.00+0.25*i,i=0..31)
     ,`if`(Eh<320.,seq(6.00+0.5*i/3,i=0..47)      ,seq(6.00+0.125*i,i=0..63))))
   ,seq(14+min(2.9/sqrt(Eh),2)*i,i=0..ceil((80-14)/min(2.9/sqrt(Eh),2)))];
hermites();
```

4. Solution of the metastable states problem

```
steps1 := [27.910, 13.658, 8.739, 6.405, 4.653, 3.603, 2.883, 2.389, 2.030, 1.754
 ,1.536, 1.358, 1.216, 1.095, .994, .908, .834, .770, .715, .665,.621, .582, .546, .515, .486
 , .460, .435, .414, .393, .374,.357, .341, .326, .342, .305, .276, .252, .233, .217, .204
 ,.192, .181, .172, .164, .157, .150, .144, .138, .133, .128, .124, .119];

L:=25;
zmesh1:=[1.90,1.95,2.00,2.07,2.15,2.22,2.30,2.36,2.42,seq(2.50+0.1*i,i=0..14)
,`if`(L>44,seq(4.00+0.1*i,i=0..19),seq(4.00+0.2*i,i=0..9))
,`if`(L<24,seq(6.00+0.5*i,i=0..15),`if`(L<37,seq(6.00+0.25*i,i=0..31)
  ,`if`(L<43,seq(6.00+0.5*i/3,i=0..47),seq(6.00+0.125*i,i=0..63))))
,seq(14+steps1[max(L,9)]*i,i=0..ceil((80-14)/steps1[max(L,9)]))];
```

```
for i from nops(zmesh1)-1 to 2 by -1 do
 if(vpot(zmesh1[i])>vpot(zmesh1[i+1]) and vpot(zmesh1[i])>vpot(zmesh1[i-1])) then zmax1:=zmesh1[i];imax:=i+2; fi;
 if(vpot(zmesh1[i])<vpot(zmesh1[i+1]) and vpot(zmesh1[i])<vpot(zmesh1[i-1])) then zmin1:=zmesh1[i]; fi;
od;

keypot:=1;Emin:=max(0,vpot(zmin1));Emax:=vpot(zmax1);nexec:=99;normtp:=0;zmesh:=zmesh1[1..imax];DirR:=2;
hermites(); read "ev99proc.dat":

for j from 1 to Ecur99 do
   keypot:=3;mukopt:=1:mukc:=0;nexec:=1000+10*L+j; zmesh:=zmesh1;DirR:=3;  Eh:=EIGV99[j];
  EIGFinit:=proc(z,ndiff) EIGF99(j,z,ndiff) end:
  RBoundR:=expand(convert(series(L/(zmesh[-1])
    -sqrt(EEh/sc2)*HankelH1(L+3/2,sqrt(EEh/sc2)*zmesh[-1])
                  /HankelH1(L+1/2,sqrt(EEh/sc2)*zmesh[-1]),EEh=Eh),polynom));
  hermites();
od:
```

REFERENCES

1. Patkowski, K., Špirko, V., and Szalewicz, K. "On the elusive twelfth vibrational state of beryllium dimer, Science 326, 1382-1384 (2009)
2. Mitin, A.V. "Ab initio calculations of weakly bonded He_2 and Be_2 molecules by MRCI method with pseudo-natural molecular orbitals, Int. J. Quantum Chem. 111 2560–2567, (2011).
3. Mitin, A.V. "Unusual chemical bonding in the beryllium dimer and its twelve vibrational levels, Chem. Phys. Lett. 682, 30-33 (2017)
4. Lesiuk, M., Przybytek, M., Balcerzak, J.G., Musial, M. Moszynski, R. "Ab initio potential energy curve for the ground state of beryllium dimer, J. Chem. Theory Comput. 15, 2470-2480 (2019)
5. Meshkov, V.V., Stolyarov, A.V., Heaven, M.C., et al. "Direct-potential-fit analyses yield improved empirical potentials for the ground $X^1\Sigma_g^+$ state of Be_2, J. Chem. Phys. 140, 064315-1-8 (2014)
6. Merritt,J.M., Bondybey, V.E., Heaven, M.C. "Beryllium dimer – caught in the act of bonding, Science 324 (5934), 1548-1551 (2009)
7. Gusev, A., Chuluunbaatar, O., Vinitsky, S., et al. "On rotational-vibrational spectrum of diatomic beryllium molecule, Proceedings of SPIE, 11066, 1106619 (2019)
8. Sheng, X.W., Kuang, X.Y., Li, P., Tang, K.T. "Analyzing and modeling the interaction potential of the ground-state beryllium dimer, Phys. Rev. A 88, 022517 (2013)
9. Porsev S.G., Derevianko, A. "High-accuracy calculations of dipole, quadrupole, and octupole electric dynamic polarizabilities and van der Waals coefficients C_6, C_8, and C_{10} for alkaline-earth dimers, JETP, 102, 195-205 (2006)
10. Derbov, V., Chuluunbaatar, G., Gusev, A., Chuluunbaatar, O., Vinitsky, S., et al., On calculations of metastable and Rydberg states of diatomic beryllium molecule and antiprotonic helium atom Proc. of SPIE 11458, p. 114580Q (2020).
11. Chuluunbaatar, O., Gusev, A.A., Vinitsky, S.I., Abrashkevich, A.G. "ODPEVP: A program for computing eigenvalues and eigenfunctions and their first derivatives with respect to the parameter of the parametric self-adjoined Sturm-Liouville problem, Comput. Phys. Commun. 181, 1358-1375 (2009)
12. Gusev, A.A., Chuluunbaatar, O., Vinitsky, S.I., et al. talk in MAPLE 2020 conference https://www.maplesoft.com/mapleconference/
13. KANTBP 5M program will be publisehd as open code in JINRLIB (2021).
14. JINRLIB (2015) http://wwwinfo.jinr.ru/programs/jinrlib/kantbp4m/indexe JINRLIB (2015) http://wwwinfo.jinr.ru/programs/jinrlib/kantbp4m
15. Gusev, A.A., Chuluunbaatar, O., Vinitsky, S.I., et al. "Symbolic-numerical solution of boundary-value problems with self-adjoint second-order differential equation using the finite element method with interpolation Hermite polynomials, Lecture Notes in Computer Science 8660, 138-154 (2014)
16. Gusev, A.A., Hai, L.L., Chuluunbaatar, O., et al. "Symbolic-numeric solution of boundary-value problems for the Schrodinger equation using the finite element method: scattering problem and resonance states, Lecture Notes in Computer Science 9301, pp. 182-197 (2015)
17. https://www.nist.gov/pml/atomic-spectroscopy-databases
18. M.L. Goldberger and K.M. Watson, Collision Theory, John Wiley & Sons, Inc. NY. 1964.